Numerical Modeling of Coupled Thermo-elasticity with Relaxation Times in Rotating FGAPs Subjected to a Moving Heat Source

Mohamed Abdelsabour Fahmy*, †

*** Jummum University College**
Umm Al-Qura University
Alazizya, behind Alsalam Souq, 21955 Makkah, Saudi Arabia.
e-mail: maselim@uqu.edu.sa

† Faculty of Computers and Informatics
Suez Canal University
New Campus, 4.5 Km, Ring Road, El Salam District, 41522 Ismailia, Egypt.
e-mail: Mohamed_fahmy@ci.suez.edu.eg

Abstract. The time-stepping DRBEM modeling was proposed to study the 2D dynamic response of functionally graded anisotropic plate (FGAP) subjected to a moving heat source. The FGAP is assumed to be graded through the thickness. A Gaussian distribution of heat flux using a moving heat source with a conical shape is used for analyzing the temperature profiles. The main aim of this paper is to evaluate the difference between Green and Lindsay (G-L) and Lord and Shulman (L-S) theories of coupled thermo-elasticity in rotating FGAP subjected to a moving heat source. The accuracy of the proposed method was examined and confirmed by comparing the obtained results with those known previously.

Keywords: Thermo-elasticity; Functionally Graded Anisotropic Plates; Boundary Element Method.

1. Introduction

Biot [1] proposed the classical coupled thermo-elasticity (CCTE) theory to overcome the paradox inherent in the classical uncoupled thermo-elasticity (CUTE) theory that elastic changes have no effect on temperature. The heat equations for both theories are a diffusion type predicting infinite speeds of propagation for heat waves contrary to physical observations. A flux rate term into Fourier law of heat conduction is incorporated by Lord and Shulman (L-S) [2], who proposed an extended thermo-elasticity theory (ETE) which is also called as the generalized thermo-elasticity theory with one relaxation time. Another thermo-elasticity theory that admits the second sound effect is reported by Green and Lindsay (G-L) [3], who developed a temperature-rate-dependent thermo-elasticity theory (TRDTE) which is also called the generalized thermo-elasticity theory with two relaxation times by introducing two relaxation times that relate the stress and entropy to the temperature.

Functionally graded Plates (FGPs) are a type of non-homogeneous composites and the transient thermo-elastic problems for these non-homogeneous composites become important, and there are several studies concerned with these problems, such as Skouras et al. [4], Mojdehi et al. [5], Zhou et al. [6], Loghman et al. [7], Sun and Luo [8] and Mirzaei and Dehghan [9] which are papers involving functionally graded materials.

In recent years, the dynamical problem of thermo-elasticity for functionally graded anisotropic plates (FGAPs) becomes more important due to its many applications in modern aeronautics, astronautics, earthquake engineering, soil dynamics, mining engineering, plasma physics, nuclear reactors and high-energy particle accelerators, for instance. Abd-Alla [10] obtained the relaxation effects on reflection of generalized magneto-thermo-elastic waves. Abd-Alla and Al-Dawy [11] obtained the relaxation effects on Rayleigh waves in generalized thermoelastic media. Abbas and Abd-Alla [12, 13] studied generalized thermoelastic problems for an infinite fibre-reinforced anisotropic plate. Xia, et al. [14] used a time domain finite element method to solve dynamic response of two-dimensional generalized thermoelastic coupling problem subjected to a moving heat source based on Lord and Shulman theory with one thermal relaxation time

It is hard to find the analytical solution of a problem in a general case, therefore, an important number of engineering and mathematical papers devoted to the numerical solution have studied the overall behavior of such materials (see, e.g., El-Naggar et al. [15, 16], Abd-Alla et al. [17-19], Qin [20], Sladek et al. [21], Tian et al. [22], Fahmy [23-28], Fahmy and El-Shahat [29], Othman and Song, [30], Davi and Milazzo [31], Hou et al. [32], [Abreu et al. [33], Espinosa and Mediavilla, [34].

The advantages in the boundary element method (BEM) arises from the fact that the BEM can be regarded as boundary–based method that uses the boundary integral equation formulations where only the boundary of the domain of the partial differential equation (PDE) is required to be meshed. But in the domain-based methods such the finite element method (FEM), finite difference method (FDM) and element free method (EFM) that use ordinary differential equation (ODE) or PDE formulations, where the whole domain of the PDE requires discretisation. Thus the dimension of the problem is effectively reduced by one, that is, surfaces for three–dimensional (3D) problems or curves for two-dimensional (2D) problems. And the equation governing the infinite domain is reduced to an equation over the finite boundary. Also, the BEM can be applied along with the other domain-based methods to verify the solutions to the problems that do not have available analytical solutions. Presence of domain integrals in the formulation of the BEM dramatically decreases the efficiency of this technique. One of the most widely used methods for converting the domain integral into a boundary one is the so-called dual reciprocity boundary element method (DRBEM) which was initially developed by Nardini and Brebbia [35] in the context of two-dimensional (2D) elastodynamics and has been extended to deal with a variety of problems wherein the domain integral may account for linear-nonlinear static-dynamic effects. A more extensive historical review and applications of dual reciprocity boundary element method may be found in [Brebbia et al. [36], Wrobel and Brebbia [37], Partridge and Brebbia [38], Partridge and Wrobel [39] and Fahmy [40-47]].

The main objective of this paper is to study the model of two-dimensional equations of coupled thermo-elasticity with one and two relaxation times in rotating FGAPs subjected to a moving heat source. A predictor-corrector time integration algorithm was implemented for use with the DRBEM to obtain the solution for the temperature and displacement components. The accuracy of the proposed method was examined and confirmed by comparing the obtained results with the finite element method (FEM) results known before.

2. Governing equations of the FGAP

Consider a Cartesian coordinate system $Oxyz$ as shown in Fig. 1. We shall consider a rotating functionally graded anisotropic plate occupies the region $R = \{(x, y, z): 0 < x < \gamma, 0<y<\beta, 0<z<\alpha$ with the boundary C and the material is functionally graded along the thickness direction Ox. Thus, the governing equations of Coupled Thermo-elasticity with Relaxation Times can be written in the following form:

$$\sigma_{ab,b} - \rho(x+1)^m \omega^2 x_a = \rho(x+1)^m \ddot{u}_a, \tag{1}$$

$$\sigma_{ab} = (x+1)^m \left[C_{abfg} u_{f,g} - \beta_{ab}\left(T - T_0 + \tau_1 \dot{T}\right)\right], \tag{2}$$

$$k_{ab} T_{,ab} = \beta_{ab} T_0 \dot{u}_{a,b} + \rho c (x+1)^m \left[\dot{T} + \tau_2 \ddot{T}\right] - Q. \tag{3}$$

where σ_{ab} is the mechanical stress tensor, u_k is the displacement, T is the temperature, C_{abfg} and β_{ab} are respectively, the constant elastic moduli and stress-temperature coefficients of the anisotropic medium, ω is the uniform angular velocity, k_{ab} are the thermal conductivity coefficients satisfying the symmetry relation $k_{ab} = k_{ba}$ and the strict inequality $(k_{12})^2 - k_{11}k_{22} < 0$ holds at all points in the medium, ρ is the density, c is the specific heat capacity, τ is the time, τ_1 and τ_2 are mechanical relaxation times, Q is the moving heat source.

3. 3. Numerical implementation

Making use of (2), we can write (1) as follows

$$L_{gb} u_f = \rho \ddot{u}_a - \left(D_a T + \Lambda D_{a1f} u_f - \rho \omega^2 x_a\right) = f_{gb}, \tag{4}$$

The field equations can now be written in operator form as follows

$$L_{gb} u_f = f_{gb}, \tag{5}$$

$$L_{ab} T = f_{ab}, \tag{6}$$

where the operators L_{gb}, f_{gb}, L_{ab} and f_{ab} are defined as follows

$$L_{gb} = D_{abf} \frac{\partial}{\partial x_b}, \qquad f_{gb} = \rho \ddot{u}_a - \left(D_a T + \Lambda D_{a1f} u_f - \rho \omega^2 x_a\right) \tag{7}$$

$$D_{abf} = C_{abfg} \varepsilon, \varepsilon = \frac{\partial}{\partial x_g}, \Lambda = \frac{m}{x+1}, D_a = -\beta_{ab}\left(\frac{\partial}{\partial x_b} + \delta_{b1}\Lambda + \tau_1\left(\frac{\partial}{\partial x_b} + \Lambda\right)\frac{\partial}{\partial \tau}\right)$$

$$L_{ab} = k_{ab} \frac{\partial}{\partial x_a} \frac{\partial}{\partial x_b}, \qquad f_{ab} = \rho c (x+1)^m \left[\dot{T} + \tau_2 \ddot{T}\right] + \beta_{ab} T_0 \dot{u}_{a,b} - Q. \tag{8}$$

Using the weighted residual method (WRM), the differential equation (5) is transformed into an integral equation

$$\int_R \left(L_{gb} u_f - f_{gb}\right) u_{da}^* \, dR = 0. \tag{9}$$

Now, by choosing the fundamental solution u_{df}^* as the weighting function as follows

$$L_{gb} u_{df}^* = -\delta_{ad} \delta(x, \xi). \tag{10}$$

The corresponding traction field can be written as

$$t_{da}^* = C_{abfg} u_{df,g}^* n_b. \tag{11}$$

where ξ is the load point and n_b is the unit normal vector to the surface.

The thermo-elastic traction vector can be written as follows

$$t_a = \frac{\bar{t}_a}{(x+1)^m} = \left(C_{abfg} u_{f,g} - \beta_{ab}\left(T - T_0 + \tau_1 \dot{T}\right)\right) n_b. \tag{12}$$

Applying integration by parts to (9) using the sifting property of the Dirac distribution, and using equations (10) and (12), we can write the following elastic integral representation formula

$$u_d(\xi) = \int_C (u^*_{da} t_a - t^*_{da} u_a + u^*_{da} \beta_{ab} T n_b)\, dC - \int_R f_{gb} u^*_{da} dR. \tag{13}$$

The fundamental solution T^* of the thermal operator L_{ab}, defined by

$$L_{ab} T^* = -\delta(x, \xi). \tag{14}$$

By implementing the WRM and integration by parts, the differential equation (6) is transformed into the thermal reciprocity equation

$$\int_R (L_{ab} T T^* - L_{ab} T^* T) dR = \int_C (q^* T - q T^*) dC, \tag{15}$$

Where the heat fluxes are as follows:

$$q = -k_{ab} T_{,b} n_a, \tag{16}$$

$$q^* = -k_{ab} T^*_{,b} n_a. \tag{17}$$

The thermal integral representation formula from (16) may be written as

$$T(\xi) = \int_C (q^* T - q T^*) dC - \int_R f_{ab} T^* dR. \tag{18}$$

The integral representation formulae of elastic and thermal fields (13) and (18) can be combined to form a single equation as follows

$$\begin{bmatrix} u_d(\xi) \\ T(\xi) \end{bmatrix} = \int_C \left\{ -\begin{bmatrix} t^*_{da} & -u^*_{da} \beta_{ab} n_b \\ 0 & -q^* \end{bmatrix} \begin{bmatrix} u_a \\ T \end{bmatrix} + \begin{bmatrix} u^*_{da} & 0 \\ 0 & -T^* \end{bmatrix} \begin{bmatrix} t_a \\ q \end{bmatrix} \right\} dC$$

$$- \int_R \begin{bmatrix} u^*_{da} & 0 \\ 0 & -T^* \end{bmatrix} \begin{bmatrix} f_{gb} \\ -f_{ab} \end{bmatrix} dR. \tag{19}$$

It is convenient to use the contracted notation to introduce generalized thermo elastic vectors and tensors, which contain corresponding elastic and thermal variables as follows:

$$U_A = \begin{cases} u_a & a = A = 1, 2, 3; \\ T & A = 4, \end{cases} \tag{20}$$

$$T_A = \begin{cases} t_a & a = A = 1, 2, 3; \\ q & A = 4, \end{cases} \tag{21}$$

$$U^*_{DA} = \begin{cases} u^*_{da} & d = D = 1, 2, 3; a = A = 1, 2, 3; \\ 0 & d = D = 1, 2, 3; A = 4; \\ 0 & D = 4; a = A = 1, 2, 3; \\ -T^* & D = 4; A = 4, \end{cases} \tag{22}$$

$$\tilde{T}^*_{DA} = \begin{cases} t^*_{da} & d = D = 1, 2, 3; a = A = 1, 2, 3; \\ -\tilde{u}^*_d & d = D = 1, 2, 3; A = 4; \\ 0 & D = 4; a = A = 1, 2, 3; \\ -q^* & D = 4; A = 4, \end{cases} \tag{23}$$

$$\tilde{u}^*_d = u^*_{da} \beta_{af} n_f. \tag{24}$$

The thermo-elastic representation formula (19) can be written in contracted notation as:

$$U_D(\xi) = \int_C \left(U^*_{DA} T_A - \tilde{T}_{DA} U_A \right) dC - \int_R U^*_{DA} S_A dR, \tag{25}$$

The vector S_A can be written in the split form as follows

$$S_A = S^0_A + S^T_A + S^u_A + S^{\dot{T}}_A + S^{\ddot{T}}_A + S^{\dot{u}}_A + S^{\ddot{u}}_A, \tag{26}$$

where

$$S_A^0 = \begin{cases} \rho\omega^2 x_a & a = A = 1,2,3; \\ Q & A = 4, \end{cases} \tag{27}$$

$$S_A^T = \omega_{AF} U_F \qquad with \quad \omega_{AF} = \begin{cases} -D_a & A = 1,2,3; F = 4; \\ 0 & otherwise, \end{cases} \tag{28}$$

$$S_A^u = -\left(D_{af} + \Lambda D_{a1f}\right)\mho U_F$$

With $\mho = \begin{cases} 1 & a = A = 1,2,3; f = F = 1,2,3; \\ 0 & otherwise, \end{cases}$ (29)

$$S_A^{\dot{T}} = -\rho c(x+1)^m \delta_{AF} \dot{U}_F \;\; with \;\; \delta_{AF} = \begin{cases} 1 & A = 4; F = 4; \\ 0 & otherwise, \end{cases} \tag{30}$$

$$S_A^{\ddot{T}} = -\rho c(x+1)^m \tau_2 \delta_{AF} \ddot{U}_F, \tag{31}$$

$$S_A^{\dot{u}} = -T_0 \text{Å} \delta_{1j} \beta_{fg} \varepsilon \dot{U}_F, \tag{32}$$

$$S_A^{\ddot{u}} = \quad \ddot{U}_F \qquad with \qquad = \begin{cases} \rho & A = 1,2,3;\; F = 1,2,3; \\ 0 & A = 4; f = F = 4. \end{cases} \tag{33}$$

The thermo-elastic representation formula (19) can be rewritten in matrix form as follows:

$$[S_A] = \begin{bmatrix} \rho\omega^2 x_a \\ Q \end{bmatrix} + \begin{bmatrix} -D_a T \\ 0 \end{bmatrix} + \begin{bmatrix} -\left(D_{af} + \Lambda D_{a1f}\right)u_f \\ 0 \end{bmatrix}$$
$$+\left(\rho c(x+1)^m\right)\begin{bmatrix} 0 \\ \dot{T} \end{bmatrix} - \rho c(x+1)^m \tau_2 \begin{bmatrix} 0 \\ \ddot{T} \end{bmatrix} - T_0 \begin{bmatrix} 0 \\ \beta_{ab}\dot{u}_{a,b} \end{bmatrix} + \begin{bmatrix} \rho\ddot{u}_a \\ 0 \end{bmatrix}. \tag{34}$$

By implementing the DRBEM to transform the domain integral in (25) to the boundary integral, the source vector S_A in the domain was approximated by the following series of given tensor functions f_{AN}^q and unknown coefficients α_N^q

$$S_A \approx \sum_{q=1}^{N} f_{AN}^q \alpha_N^q. \tag{35}$$

According to the implementation of the DRBEM, the surface of the plate has to be discretized into boundary elements, where the total number of interpolation points is $N = N_b + N_i$ in which N_b are collocation points on the boundary C and N_i are the interior points of R

Thus, the thermo-elastic representation formula (25) can be written in the following form

$$U_D(\xi) = \int_C \left(U_{DA}^* T_A - \tilde{T}_{DA}^* U_A\right) dC - \sum_{q=1}^{N} \int_R U_{DA}^* f_{AN}^q dR \, \alpha_N^q. \tag{36}$$

By applying the WRM to the following inhomogeneous elastic and thermal equations:

$$L_{gb} u_{fn}^q = f_{an}^q, \tag{37}$$

$$L_{ab} T^q = f_{pj}^q, \tag{38}$$

Where the weighting functions were chosen to be the same as the elastic and thermal fundamental solutions u_{da}^* and T^*. Then the elastic and thermal representation formulae are as follows (Fahmy [42])

$$u_{de}^q(\xi) = \int_C \left(u_{da}^* t_{ae}^q - t_{da}^* u_{ae}^q\right) dC - \int_R u_{da}^* f_{ae}^q dR, \tag{39}$$

$$T^q(\xi) = \int_C \left(q^* T^q - q^q T^*\right) dC - \int_R f^q T^* dR. \tag{40}$$

The elastic and thermal fields can be combined to form the following dual representation formulae

$$U_{DN}^{q}(\xi) = \int_{C} \left(U_{DA}^{*} T_{AN}^{q} - T_{DA}^{*} U_{AN}^{q}\right) dC - \int_{R} U_{DA}^{*} f_{AN}^{q}\, dR, \tag{41}$$

By substituting from (41) into (36), we can rewrite the dual reciprocity representation formula of coupled thermo elasticity as follows

$$U_{D}(\xi) = \int_{C} \left(U_{DA}^{*} T_{A} - \breve{T}_{DA}^{*} U_{A}\right) dC + \sum_{q=1}^{N} \left(U_{DN}^{q}(\xi) + \int_{C} \left(T_{DA}^{*} U_{AN}^{q} - U_{DA}^{*} T_{AN}^{q}\right) dC \right) \alpha_{N}^{q}. \tag{42}$$

Using the thin plate splines (TPS) of Fahmy [27], we can write the particular solution of the displacement as follows

$$U_{GN}^{q} = \begin{cases} -\dfrac{4}{\lambda^4}\left[K_0(\lambda r) + log(r) - \dfrac{r^2\, log\, r}{\lambda^2} - \dfrac{4}{\lambda^4}\right], & r > 0 \\ \dfrac{4}{\lambda^4}\left[\Upsilon + log\left(\dfrac{\lambda}{2}\right)\right] - \dfrac{4}{\lambda^4}\,, & r = 0 \end{cases} \tag{43}$$

where K_0 is the Bessel function of the third kind of order zero, $\Upsilon = 0.5772156649015328$ is the Euler's constant and $r = \|x - \xi\|$ is the Euclidean distance between the field point x and the load point ξ.

According to the steps described in Fahmy [43], the dual reciprocity boundary integral equation (42) can be written in the following system of equations

$$\tilde{\zeta}\breve{u} - \eta\check{t} = \left(\zeta\breve{U} - \eta\breve{\wp}\right)\alpha. \tag{44}$$

Where the matrix ζ contains the fundamental solution $\mathrm{T}_{\mathrm{M}}^{*}$ and the matrix $\check{\zeta}$ contains the modified fundamental tensor $\breve{\mathrm{T}}_{\mathrm{M}}^{*}$ with the coupling term.
Using the technique was proposed by Partridge et al. [48], then the generalized displacements U_F and velocities $\dot{U}_F$ are approximated as follows

$$U_F \approx \sum_{q=1}^{N} f_{FD}^{q}(x)\gamma_{D}^{q}, \tag{45}$$

$$\dot{U}_F \approx \textstyle\sum_{q=1}^{N} f_{FD}^{q}(x)\tilde{\gamma}_{D}^{q}, \tag{46}$$

where f_{FD}^{q} are tensor functions and γ_{D}^{q} and $\tilde{\gamma}_{D}^{q}$ are unknown coefficients.
The gradients of displacement and velocity were approximated as follows

$$U_{F,g} \approx \sum_{q=1}^{N} f_{K,g}^{q}(x)\gamma_{K}^{q}, \tag{47}$$

$$\dot{U}_{F,g} \approx \sum_{q=1}^{N} f_{FD,g}^{q}(x)\tilde{\gamma}_{D}^{q}. \tag{48}$$

If these approximations are substituted into equations (5.39) (28) and (32) we obtain the corresponding approximating source terms as follows

$$S_{A}^{T} = \sum_{q=1}^{N} S_{AD}^{T,q}\,\gamma_{D}^{q}, \tag{49}$$

$$S_A^{\dot{u}} = -T_0\beta_{fg}\varepsilon\sum_{q=1}^{N} S_{AD}^{\dot{u},q}\,\tilde{\gamma}_D^q, \tag{50}$$

where

$$S_{AD}^{T,q} = S_{AF} f_{FD,g}^{q}, \tag{51}$$

$$S_{AD}^{\dot{u},q} = S_{FA} f_{FD,g}^{q}. \tag{52}$$

Applying the point collocation procedure of Gaul, et al. [49] to equations (35), (45) and (46) we have the following system of equations

$$\breve{S} = J\alpha, \qquad U = J'\gamma, \qquad \dot{U} = J'\tilde{\gamma}. \tag{53}$$

Similarly, the application of the point collocation procedure to the source terms equations (29), (30), (31), (33), (49) and (50) leads to the following system of equations

$$\breve{S}^u = -\left(D_{af} + \Lambda D_{a1f}\right)\mho U_F \qquad \textit{With}$$

$$\mho = \begin{cases} 1 & a = A = 1,2,3;\, f = F = 1,2,3; \\ 0 & otherwise, \end{cases} \tag{54}$$

$$\breve{S}^{\dot{T}} = \rho c(x+1)^m \delta_{AF}\dot{U}, \tag{55}$$

$$\breve{S}^{\ddot{T}} = -c\rho(x+1)^m \tau_2 \delta_{AF}\ddot{U}, \tag{56}$$

$$\breve{S}^{\ddot{u}} = \tilde{A}\ddot{U}, \tag{57}$$

$$\breve{S}^{T} = \mathcal{B}^T\gamma, \tag{58}$$

$$\breve{S}^{\dot{u}} = -T_0\beta_{fg}\varepsilon\mathcal{B}^{\dot{u}}\tilde{\gamma}. \tag{59}$$

Solving the system (53) for α, γ and $\tilde{\gamma}$ yields

$$\alpha = J^{-1}\breve{S}, \qquad \gamma = J'^{-1}U, \qquad \tilde{\gamma} = J'^{-1}\dot{U}, \tag{60}$$

Now, the coefficients α can be expressed in terms of nodal values of the unknown displacements U, velocities $\breve{\dot{U}}$ and accelerations $\breve{\ddot{U}}$ as follows:

$$\alpha = J^{-1}(\breve{S}^0 + \left[\mathcal{B}^T J'^{-1} - \left(D_{af} + \Lambda D_{a1f}\right)\mho\right]U + \left[\rho c(x+1)^m\delta_{AF} - T_0\beta_{fg}\varepsilon\mathcal{B}^{\dot{u}}J'^{-1}\right]\dot{U} + \left[\tilde{A} - \rho c(x+1)^m\tau_2\delta_{AF}\right]\ddot{U}), \tag{61}$$

Where $\tilde{A}$ and $\mathcal{B}^T$ are assembled using the sub matrices [ ] and ω_{AF} respectively.

Substituting from Eq. (61) into Eq. (44), we obtain

$$M\ddot{U} + \Gamma\dot{U} + KU = \mathbb{Q}, \tag{62}$$

In which $\ddot{U}, \dot{U}, U$ and $\mathbb{Q}$ represent the acceleration, velocity, displacement and external force vectors, respectively, V, M, Γ and K represent the volume, mass, damping and stiffness matrices, respectively, as follows:

$$V = \left(\eta\breve{\wp} - \zeta\breve{U}\right)J^{-1}, \qquad M = V\left[\tilde{A} - c\rho(x+1)^m\tau_2\delta_{AF}\right],$$

$$\Gamma = V\left[\rho c(x+1)^m\delta_{AF} - T_0\beta_{fg}\varepsilon\mathcal{B}^{\dot{u}}J'^{-1}\right],$$

$$K = \tilde{\zeta} + V\left[\mathcal{B}^T J'^{-1} + \left(D_{af} + \Lambda D_{a1f}\right)\mho\right], \quad \mathbb{Q} = \eta T + V\breve{S}^0, \tag{63}$$

Using the initial conditions $U(0) = U_0$, $\dot{U}(0) = V_0$. Then, from Eq. (62), we can calculate the initial acceleration vector W_0 as follows

$$MW_0 = \mathbb{Q}_0 - \Gamma V_0 - KU_0. \tag{64}$$

An implicit-explicit time integration algorithm of Hughes et al. [50, 51], was developed and implemented for use with the DRBEM. This algorithm consists in satisfying the following equations

$$M\ddot{U}_{n+1} + \Gamma^I\dot{U}_{n+1} + \Gamma^E\tilde{\dot{U}}_{n+1} + K^I U_{n+1} + K^E\tilde{U}_{n+1} = \mathbb{Q}_{n+1}, \tag{65}$$

$$U_{n+1} = \tilde{U}_{n+1} + \gamma\Delta\tau^2\ddot{U}_{n+1}, \tag{66}$$

$$\dot{U}_{n+1} = \tilde{\dot{U}}_{n+1} + \alpha\Delta\tau\ddot{U}_{n+1}, \tag{67}$$

Where the superscripts I and E denote, respectively, to the implicit and explicit parts and

$$\widetilde{U}_{n+1} = U_{n+1} + \Delta\tau\dot{U}_n + (1-2\gamma)\frac{\Delta\tau^2}{2}\ddot{U}_n, \tag{68}$$

$$\widetilde{\dot{U}}_{n+1} = \dot{U}_n + (1-\alpha)\Delta\tau\ddot{U}_n, \tag{69}$$

Where we used the quantities $\widetilde{U}_{n+1}$ and $\widetilde{\dot{U}}_{n+1}$ to denote the predictor values, and U_{n+1} and $\dot{U}_{n+1}$ to denote the corrector values. It is easy to recognize that the equations (66)-(69) correspond to the Newmark formulas [52].

At each time-step, equations (65)-(69), constitute an algebraic problem in terms of the unknown accelerations $\ddot{U}_{n+1}$. The first step in the code starts by forming and factoring the effective mass

$$M^* = M + \gamma\Delta\tau C^I + \gamma\Delta\tau^2 K^I. \tag{70}$$

The time step $\Delta\tau$ must be constant to run this step. As the time-step $\Delta\tau$ is changed, the first step should be repeated at each new step. The second step is to form residual force

$$\mathbb{Q}^*_{n+1} = \mathbb{Q}_{n+1} - C^I\widetilde{\dot{U}}_{n+1} - C^E\widetilde{\dot{U}}_{n+1} - K^I\widetilde{U}_{n+1} - K^E\widetilde{U}_{n+1}. \tag{71}$$

The third step is to solve $M^*\ddot{U}_{n+1} = \mathbb{Q}^*_{n+1}$ using a Crout elimination algorithm [53] which fully exploits that structure in that zeroes outside the profile are neither stored nor operated upon. The fourth step is to use predictor-corrector equations (66) and (67) to obtain the corrector displacement and velocity vectors, respectively.

4. Numerical results and discussion

The Gaussian heat flux distribution $Q(x,y)$ can be expressed as

$$Q(x,y) = \frac{3Q_0}{\pi r^2}e^{\left(-\frac{3(x^2+y^2)}{r^2}\right)} \tag{72}$$

where Q_0 is heat power of the plane heat source, r is the heat source radius.

Following Rasolofosaon and Zinszner [54] monoclinic North Sea sandstone reservoir rock was chosen as an anisotropic material and physical data are as follows:

Elasticity tensor

$$C_{abfg} = \begin{bmatrix} 17.77 & 3.78 & 3.76 & 0.24 & -0.28 & 0.03 \\ 3.78 & 19.45 & 4.13 & 0 & 0 & 1.13 \\ 3.76 & 4.13 & 21.79 & 0 & 0 & 0.38 \\ 0 & 0 & 0 & 8.30 & 0.66 & 0 \\ 0 & 0 & 0 & 0.66 & 7.62 & 0 \\ 0.03 & 1.13 & 0.38 & 0 & 0 & 7.77 \end{bmatrix} GPa \tag{73}$$

Mechanical temperature coefficient

$$\beta_{ab} = \begin{bmatrix} 0.001 & 0.02 & 0 \\ 0.02 & 0.006 & 0 \\ 0 & 0 & 0.05 \end{bmatrix} \cdot 10^6\ N\ /Km^2 \tag{74}$$

Tensor of thermal conductivity is

$$k_{ab} = \begin{bmatrix} 1 & 0.1 & 0.2 \\ 0.1 & 1.1 & 0.15 \\ 0.2 & 0.15 & 0.9 \end{bmatrix} W/Km \tag{75}$$

Mass density $\rho = 2216$ kg/m^3 and heat capacity $c = 0.1$ J/(kg K). The numerical values of the temperature and displacement are obtained by discretizing the boundary into 120 elements ($N_b = 120$) and choosing 60 well-spaced out collocation points ($N_i = 60$) in the interior of the solution domain, referring to the recent work of Fahmy [55, 56].

The initial and boundary conditions considered in the calculations are

$$\text{at} = 0\ ,\ u_1 = u_2 = \dot{u}_1 = \dot{u}_2 = 0,\ T = 0 \tag{76}$$

$$\text{at } x = 0 \qquad \frac{\partial u_1}{\partial x} = \frac{\partial u_1}{\partial x} = 0, \frac{\partial T}{\partial x} = 0 \tag{77}$$

$$\text{at } x = \underline{\gamma} \qquad \frac{\partial u_1}{\partial x} = \frac{\partial u_1}{\partial x} = 0, \frac{\partial T}{\partial x} = 0 \tag{78}$$

$$\text{at } y = 0 \qquad \frac{\partial u_1}{\partial y} = \frac{\partial u_1}{\partial y} = 0, \frac{\partial T}{\partial y} = 0 \tag{79}$$

$$\text{at } y = \underline{\beta} \qquad \frac{\partial u_1}{\partial y} = \frac{\partial u_1}{\partial y} = 0, \frac{\partial T}{\partial y} = 0 \tag{80}$$

The present work should be applicable to any problems for coupled theory of thermo-elasticity in rotating FGAP. Such a technique was discussed in Fahmy et al. [57-60] who solved the special case from this study in the absence of a moving heat source. To achieve better efficiency than the technique described in Fahmy et al. [57-60], we use thin plate splines into a code, which is proposed in the current study. We extend the study of Fahmy et al. [57-60], to solve 2D in the presence of a moving heat source. Thus, it is perhaps not surprising that the numerical values obtained here are in excellent agreement with those obtained by Fahmy et al. [57-60]. The results are plotted in figures 2-4 for the Green and Lindsay (G-L) theory and plotted in figures 5–7 for the Lord and Shulman (L-S) theory to show the variation of the temperature T and the displacement components u_1 and u_2 with x coordinate. We can conclude from these figures that the temperature T and the displacement u_1 decrease with increasing x and the displacement u_2 increases with increasing x for the two theories. It has been found that the comparison between these theories evaluates the effect of second thermal relaxation time taken by Green and Lindsay. These results obtained with the DRBEM have been compared graphically with those obtained using the finite element method (FEM) method of Xia et al. [14]. It can be seen from these figures that the DRBEM results are in excellent agreement with the results obtained by FEM, thus confirming the accuracy of the DRBEM.

5. **Conclusion**

A predictor-corrector implicit-explicit time integration algorithm was developed and implemented for use with the DRBEM to obtain the solution for the temperature and displacement fields of the two-dimensional problem of coupled thermo-elasticity with one and two relaxation times in rotating FGAP subjected to a moving heat source with a conical shape. The results had been shown the difference between Green and Lindsay (G-L) and Lord and Shulman (L-S) theories of coupled thermo-elasticity in rotating FGAP subjected to a moving heat source. The accuracy of the proposed method was examined and confirmed by comparing the obtained results with the FEM obtained results. It can be seen from these figures that the DRBEM results are in excellent agreement with the results obtained by FEM

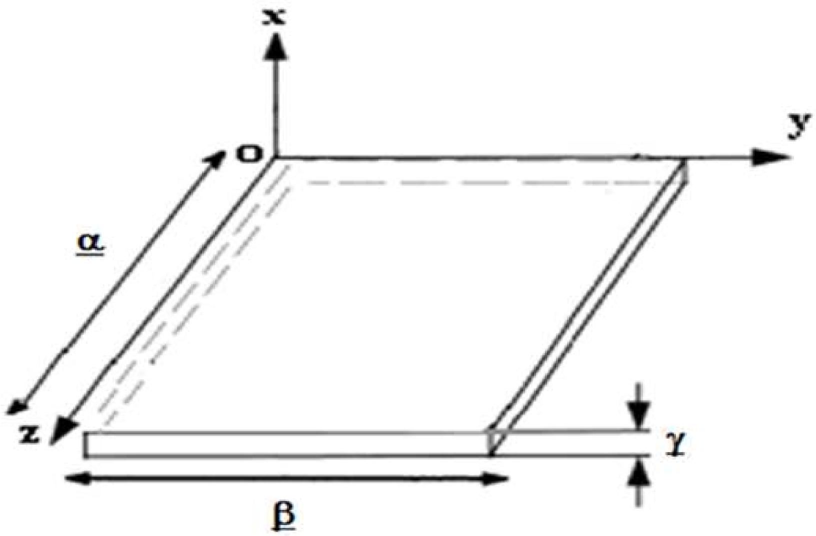

Fig. 1. The coordinate system of the FGAP.

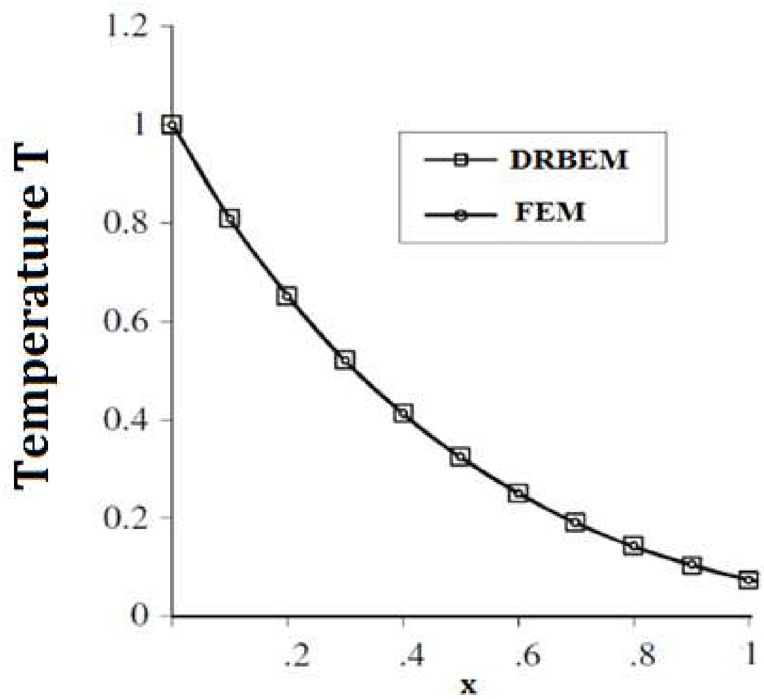

Fig. 2. Temperature distribution for G-L theory.

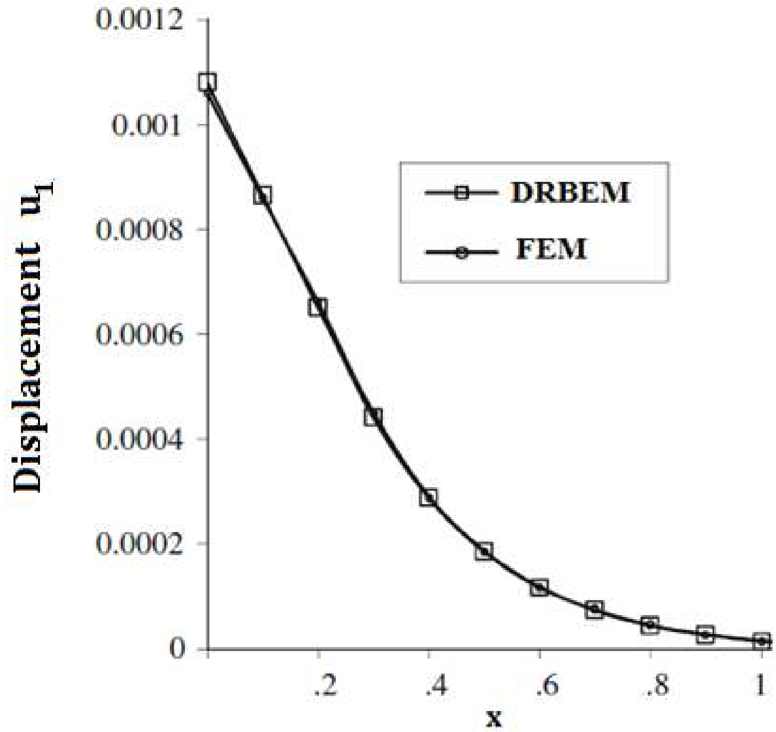

Fig. 3. Displacement distribution for G-L theory.

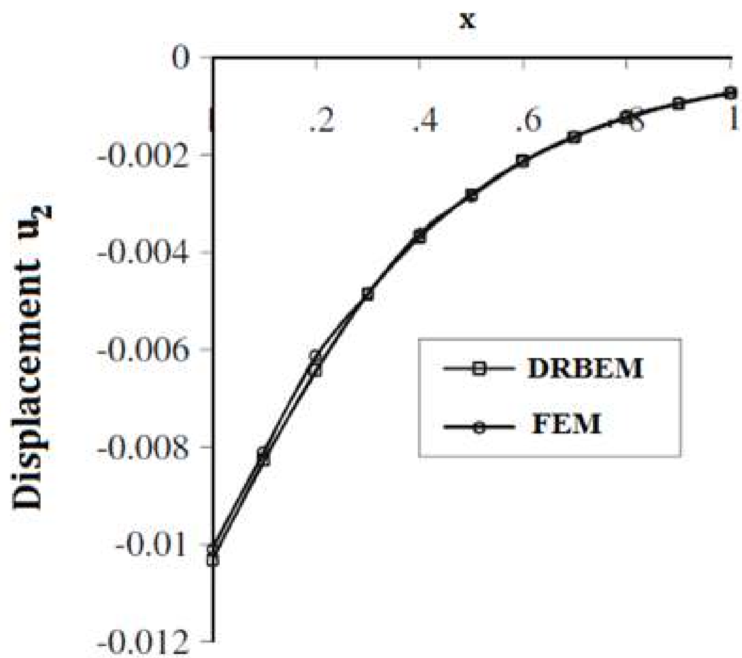

Fig. 4. Displacement distribution for G-L theory.

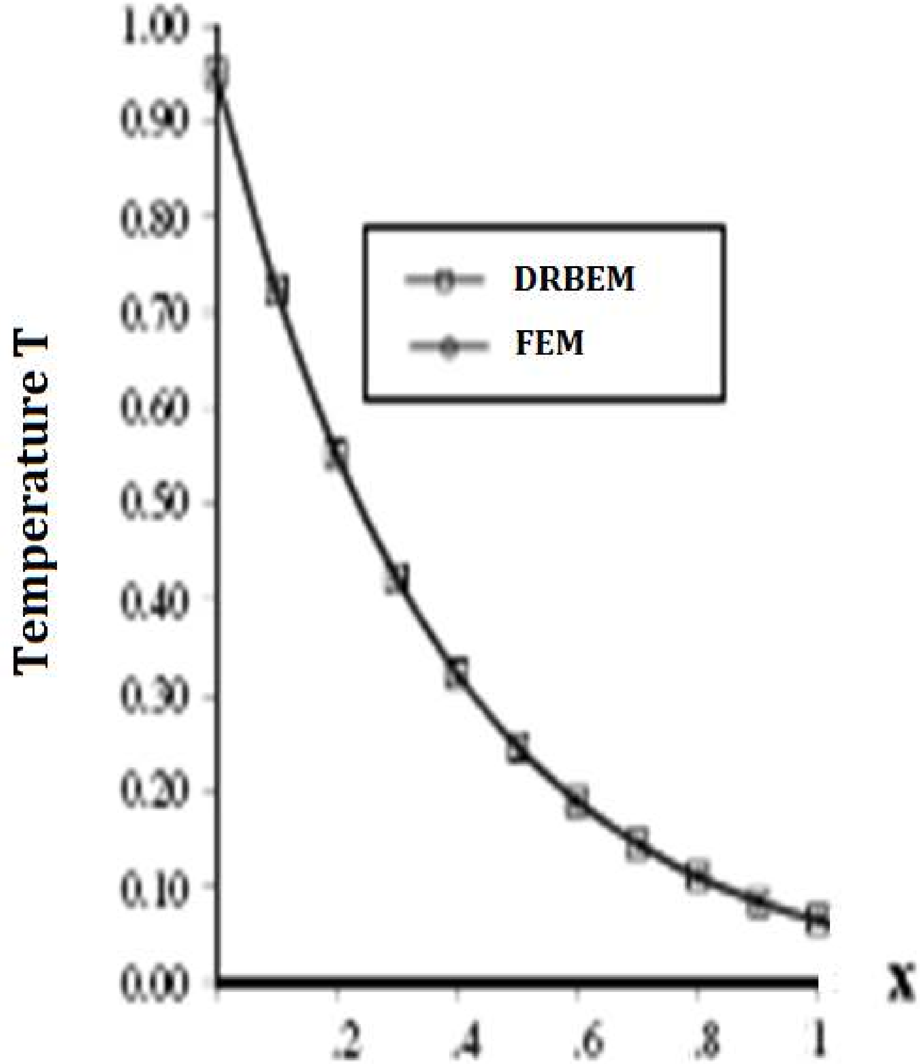

Fig. 5. Temperature distribution for L-S theory.

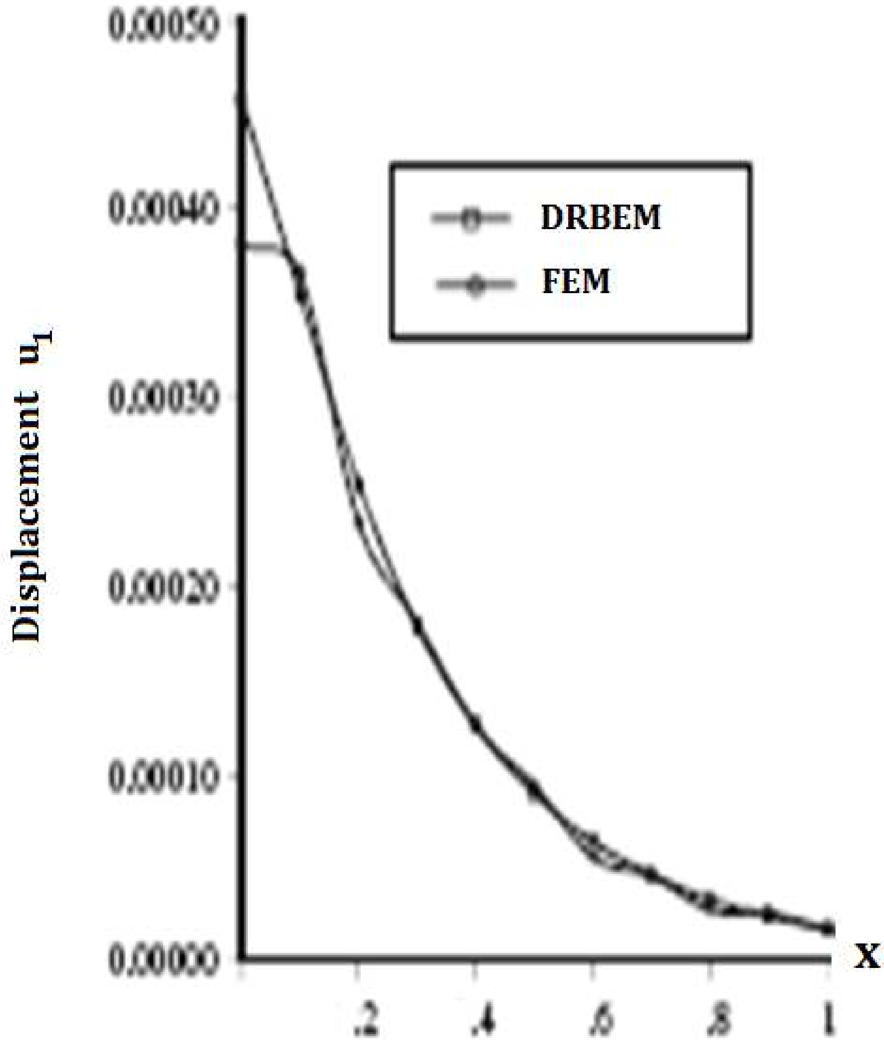

Fig. 6. Displacement distribution for L-S theory.

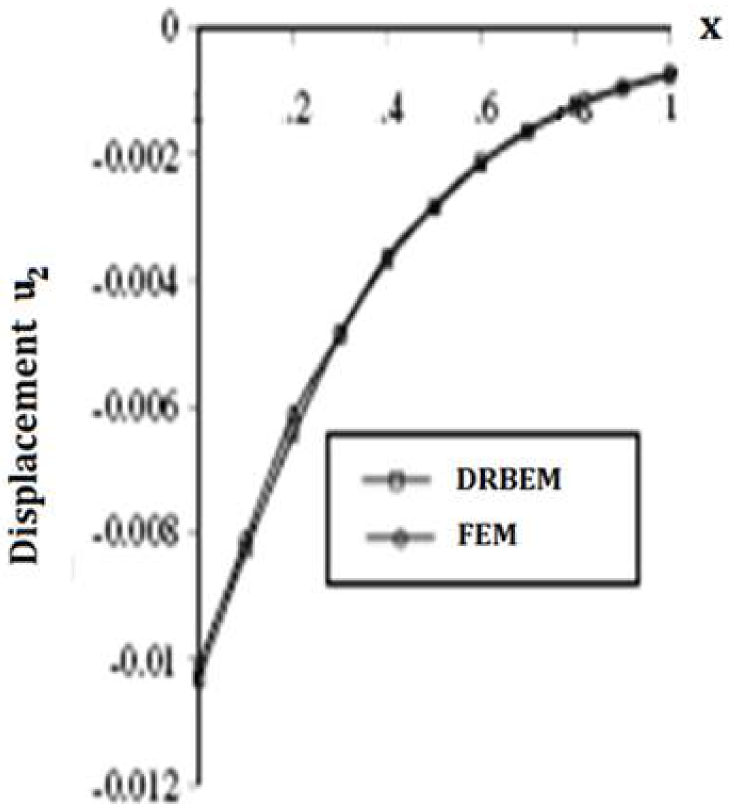

Fig. 7. Displacement distribution for L-S theory.

References

[1] Biot MA. Thermo-elasticity and irreversible thermodynamics, J. Appl. Phys. 1956;27: 240-253.

[2] Lord HW, Shulman YA. Generalized dynamical theory of thermo-elasticity, J. Mech. Phys. Solids. 1967;15:299-309.

[3] Green AE, Lindsay KA. Thermo-elasticity J. Elast. 1972;2:1-7.

[4] Skouras ED, Bourantas GC, Loukopoulos VC, Nikiforidis GC. Truly meshless localized type techniques for the steady-state heat conduction problems for isotropic and functionally graded materials, Eng. Anal. Boundary Elem. 2011;35:452-464.

[5] Mojdehi AR, Darvizeh A, Basti A, Rajabi H. Three dimensional static and dynamic analysis of thick functionally graded plates by the meshless local Petrov-Galerkin (MLPG) method, Eng. Anal. Boundary Elem. 2011;35:1168-1180.
[6] Zhou FX, Li SR, Lai YM. Three-Dimensional Analysis for Transient Coupled Thermoelastic Response of a Functionally Graded Rectangular Plate, J. of Sound and Vibration 2011;330:3990–4001.
[7] Loghman A, Aleayoub SMA, Sadi MH. Time-dependent magnetothermoelastic creep modeling of FGM spheres using method of successive elastic solution, Appl. Math. Modell, 2012;36:836-845.
[8] Sun D, Luo SN. Wave Propagation and Transient Response of a Functionally Graded Material Plate under a Point Impact Load in Thermal Environments, Appl. Mathematical Modelling. 2012;36:444–462.
[9] Mirzaei D, Dehghan M. New implementation of MLBIE method for heat conduction analysis in functionally graded materials, Eng. Anal. Boundary Elem. 2012;36:511-519.
[10] Abd-Alla AN. Relaxation effects on reflection of generalized magneto-thermo-elastic waves, Mechanics Research Communications 2000;27:591–600.
[11] Abd-Alla AN, Al-Dawy AAS. Thermal relaxation times effect on Rayleigh waves in generalized thermoelastic media, Journal of Thermal Stresses 2001;24:367-382.
[12] Abbas IA, Abd-Alla, AN. A study of generalized thermoelastic interaction in an infinite fibre-reinforced anisotropic plate containing a circular hole, Acta Physica Polonica A 2011;119:814-818.
[13] Abbas IA., Abd-Alla AN. Effect of initial stress on a fiber-reinforced anisotropic thermoelastic thick plate, International Journal of Thermophysics 2011;32:1098-1110.
[14] Xia R, Tian X, Shen Y. Dynamic response of two-dimensional generalized thermoelastic coupling problem subjected to a moving heat source, Acta Mechanica Solida Sinica 2014;27:300-305.
[15] El-Naggar AM, Abd-Alla AM, Fahmy MA, Ahmed SM. Thermal stresses in a rotating non-homogeneous orthotropic hollow cylinder, Heat Mass Transfer. 2002;39:41-46.
[16] El-Naggar AM, Abd-Alla AM, Fahmy MA. The propagation of thermal stresses in an infinite elastic slab, Appl. Math. Comput, 2004;157:307-312.
[17] Abd-Alla AM, El-Naggar AM, Fahmy MA. Magneto-thermoelastic problem in non-homogeneous isotropic cylinder, Heat Mass Transfer 2003;39:625-629.
[18] Abd-Alla AM, Fahmy MA, El-Shahat TM. Magneto-thermo-elastic stresses in inhomogeneous anisotropic solid in the presence of body force, Far East J. Appl. Math., 2007;27:499-516.
[19] Abd-Alla AM, Fahmy MA, El-Shahat TM. Magneto-thermo-elastic problem of a rotating non-homogeneous anisotropic solid cylinder, Arch. Appl. Mech. 2008;78:135-148.
[20] Qin QH. 2D Green's functions of defective magnetoelectroelastic solids under thermal loading, Eng. Anal. Boundary Elem. 2005;29:577-585.
[21] Sladek V, Sladek J, Tanaka M, Zhang Ch. Local integral equation method for potential problems in functionally graded anisotropic materials, Eng. Anal. Boundary Elem. 2005;29:829-843.
[22] Tian X, Shen Y, Chen C, He T. A direct finite element method study of generalized thermoelastic problems, International Journal of Solids and Structures. 2006;43:2050-2063.
[23] Fahmy MA. Effect of initial stress and inhomogeneity on magneto-thermo-elastic stresses in a rotating anisotropic solid, JP J. Heat Mass Transfer 2007;1:93-112.
[24] Fahmy MA. Thermoelastic stresses in a rotating non-homogeneous anisotropic body," Numer. Heat Transfer, Part A 2008;53:1001-1011.
[25] Fahmy MA. Thermal stresses in a spherical shell under three thermoelastic models using FDM, Int. J. Numer. Methods Appl., 2009;2:123-128.
[26] Fahmy MA. Finite difference algorithm for transient magneto-thermo-elastic stresses in a non-homogeneous solid cylinder. Int. J. Mater. Eng. Technol., 2010;3:87-93.

[27] Fahmy MA. Influence of inhomogeneity and initial stress on the transient magneto-thermo-visco-elastic stress waves in an anisotropic solid, World J. Mech., 2011;1:256-265.
[28] Fahmy MA. Numerical modeling of transient magneto-thermo-viscoelastic waves in a rotating nonhomogeneous anisotropic solid under initial stress, Int. J. Model. Simul. Sci. Comput., 2012;3:125002.
[29] Fahmy MA, El-Shahat TM, The effect of initial stress and inhomogeneity on the thermoelastic stresses in a rotating anisotropic solid,“ Arch. Appl. Mech., 2008;78:431-442.
[30] Othman MIA, Song Y. Effect of rotation on plane waves of generalized electro-magneto-thermoviscoelasticity with two relaxation times, Appl. Math. Modell., 2008;32:811–825.
[31] Davì G, Milazzo A. A regular variational boundary model for free vibrations of magneto-electro-elastic structures, Eng. Anal. Boundary Elem. 2011;35:303-312.
[32] Hou PF, He S, Chen CP. 2D general solution and fundamental solution for orthotropic thermoelastic materials, Eng. Anal. Boundary Elem. 2011;35:56-60.
[33] Abreu AI, Canelas A, Sensale B, Mansur WJ. CQM-based BEM formulation for uncoupled transient quasistatic thermo-elasticity analysis,“ Eng. Anal. Boundary Elem. 2012;36:568-578.
[34] Espinosa JV, Mediavilla AF. Boundary element method applied to three dimensional thermoelastic contact, Eng. Anal. Boundary Elem. 2012;36:928-933.
[35] Nardini D, Brebbia CA. A new approach to free vibration analysis using boundary elements, in: C. A. Brebbia (Eds.), Boundary elements in engineering, Springer, Berlin, 312-326; 1982.
[36] Brebbia CA, Telles JCF, Wrobel L. Boundary element techniques in Engineering, (Springer-Verlag, New York); 1984.
[37] Wrobel LC, Brebbia CA. The dual reciprocity boundary element formulation for nonlinear diffusion problems, Comput. Methods Appl. Mech. Eng. 1987;65:147-164.
[38] Partridge PW, Brebbia CA. Computer implementation of the BEM dual reciprocity method for the solution of general field equations, Commun. Appl. Numer. Methods, 6:83-92, 1990.
[39] Partridge PW, Wrobel LC. The dual reciprocity boundary element method for spontaneous ignition. Int. J. Numer. Methods Eng. 1990;30:953–963.
[40] Fahmy MA. Application of DRBEM to non-steady state heat conduction in non-homogeneous anisotropic media under various boundary elements, Far East J. Math. Sci., 2010;43:83-93.
[41] Fahmy MA. A time-stepping DRBEM for magneto-thermo-viscoelastic interactions in a rotating nonhomogeneous anisotropic solid,“ Int. J. Appl. Mech 2011;3:1-24.
[42] Fahmy MA. A time-stepping DRBEM for the transient magneto-thermo-visco-elastic stresses in a rotating non-homogeneous anisotropic solid, Eng. Anal. Boundary Elem. 2012;36:335-345.
[43] Fahmy MA. Transient magneto-thermo-elastic stresses in an anisotropic viscoelastic solid with and without moving heat source, Numer. Heat Transfer, Part A. 2012;61:547-564.
[44] Fahmy MA. Transient magneto-thermoviscoelastic plane waves in a non-homogeneous anisotropic thick strip subjected to a moving heat source, Appl. Math. Modell, 2012;36:4565-4578.
[45] Fahmy MA. Transient magneto-thermo-viscoelastic stresses in a rotating nonhomogeneous anisotropic solid with and without a moving heat source, J. Eng. Phys. Thermophys, 2012;85:874-880.
[46] Fahmy MA. The DRBEM solution of the generalized magneto-thermo-viscoelastic problems in 3D anisotropic functionally graded solids, Proceeding of V International conference on coupled problems in science and engineering, Ibiza, Spain, pp. 862-872; 2013.
[47] Fahmy MA. Boundary Element Solution of 2D Coupled Problem in Anisotropic Piezoelectric FGM Plates, Proceedings of the VI International Conference on Computational Methods for Coupled Problems in Science and Engineering, Venice. Italy. pp. 382-391; 2015.
[48] Partridge PW, Brebbia CA, Wrobel LC. The dual reciprocity boundary element method, (Computational Mechanics Publications, Boston, Southampton); 1992.
[49] Gaul L, Kögl M, Wagner M. Boundary element methods for engineers and scientists, (Springer-Verlag, Berlin); 2003.

[50] Hughes TJR, Liu WK. Implicit-Explicit finite element in Transient analysis: Stability theory. ASME J. Appl. Mech. 1978;45:371-374.

[51] Hughes TJR, Liu WK. Implicit-Explicit finite element in Transient analysis: Implementation and numerical examples. ASME J. Appl. Mech. 1978;45:375-378.

[52] Newmark NM. A method of computation for structural dynamics, J. Eng. Mech. Div. 1959;85:67-94.

[53] Taylor RL. Computer procedures for finite element analysis," in: O.C. Zienckiewicz (Third Edition), The finite element method, (McGraw Hill, London); 1977.

[54] Rasolofosaon PNJ, Zinszner BE. Comparison between permeability anisotropy and elasticity anisotropy of reservoir rocks, Geophys. 2002;67:230-240,.

[55] Fahmy MA. Implicit–Explicit Time Integration DRBEM for Generalized Magneto-Thermo-elasticity Problems of Rotating Anisotropic Viscoelastic Functionally Graded Solids., Engineering Analysis with Boundary Elements 2013;37:107-115.

[56] Fahmy MA. A Computerized DRBEM model for generalized magneto-thermo-visco-elastic stress waves in functionally graded anisotropic thin film/substrate structures, Latin American Journal of Solids and Structures 2014;11:386-409.

[57] Fahmy MA, Salem AM, Metwally MS, Rashid MM. Computer Implementation of the DRBEM for Studying the Generalized Thermoelastic Responses of Functionally Graded Anisotropic Rotating Plates with One Relaxation Time, International Journal of Applied Science and Technology 2013;3:130-140.

[58] Fahmy MA, Salem AM, Metwally MS, Rashid MM. Computer Implementation of the DRBEM for Studying the Classical Uncoupled Theory of Thermo-elasticity of Functionally Graded Anisotropic Rotating Plates, International Journal of Engineering Research and Applications 2013;3:1146-1154.

[59] Fahmy MA, Salem AM, Metwally MS, Rashid MM. Computer Implementation of the Drbem for Studying the Classical Coupled Thermoelastic Responses of Functionally Graded Anisotropic Plates, Physical Science International Journal 2014;4:674-685.

[60] Fahmy MA, Salem AM, Metwally MS, Rashid MM. Computer Implementation of the DRBEM for Studying the Generalized Thermo Elastic Responses of Functionally Graded Anisotropic Rotating Plates with Two Relaxation Times, British Journal of Mathematics & Computer Science 2014;4:1010-1026.